Point-of-use filter membrane selection, start-up, and conditioning for low-defect photolithography coatings

Nick Brakensiek[*a], Michael Cronin[b]
[a]Brewer Science, Inc., 2401 Brewer Drive, Rolla, MO, USA 65401
[b]Entegris, Inc., 129 Concord Rd., Billerica, MA, USA 01821

ABSTRACT

Recent innovations in device design, including FinFETs and metal gate technologies, have required similar innovation in lithographic materials and process development. Complex processes such as double patterning and multilayer imaging require new and novel material chemistries to meet the rigorous defect level requirements for successful yield. To address these complex processes, new materials for multilayer imaging, including spin-on hardmask layers and thick carbon underlayers, have been introduced. These two types of materials have different roles in the multilayer imaging scheme, and likewise the chemistries that are used in these materials are different. To evaluate the wide variety of materials, it is necessary to be able to install them on a coater-track quickly and efficiently and to ensure that the chosen filter uses the best available filtration settings to provide the best-performing material. Typically end users of point-of-use filters will install a new filter, which will be primed with the best-known method, and purge chemical until a defect baseline is reached.

This study examines the interaction between a spin-on hardmask chemistry and membrane materials, examining decreasing pore size and the differential pressure increases. Under these conditions, known issues with particles, microbubbles, or oddly timed defect excursions should be able to be avoided with the proper selection and start-up of the filter.

An Entegris IntelliGen® Mini dispense system with Impact® 2 filters was used to test different filtration settings on various filtration membranes and determine the best settings for each membrane type. These pumps have the capability to control differential pressure across the filter based upon its operating parameters. Results of this investigation will show that for the spin-on hardmask material, optimizing differential pressure across the filter by adjusting the IntelliGen® Mini operating parameters will ultimately reduce blanket coat defect levels. As well, reducing pore size yields a greater impact to reduction of post-coat defect counts.

Keywords:, defect, hardmask, spin-on carbon, carbon underlayer, trilayer, BARC, underlayer, filtration, filter priming, pump priming, membrane

1. INTRODUCTION

The continuing drive to extend Moore's Law has resulted in ever-shrinking and increasingly complex lithographic processes. These complexities have resulted in the use of many advanced imaging schemes and materials to achieve the required patterning and maintain acceptable product yields. The requirements for the most advanced schemes include more stringent constraints on line width variation, overlay tolerances, and defect density, among other factors. To achieve these requirements, multilayer imaging schemes are often used which employ many different types of underlayers from spin-on hardmasks to thick carbon underlayers.

Reducing defects in these layers is greatly dependent on the proper selection of filters as well as the priming and processing conditions used with the filter. Installing a new filter typically involves priming the filter with a best-known method and purging chemical until an acceptable defect baseline is reached.

N. Brakensiek, M. Cronin, "Point-of-use filter membrane selection, start-up, and conditioning for low-defect photolithography coatings," Proceedings of SPIE, vol. 8682, 2013.
© 2013 Society of Photo-Optical Instrumentation Engineers. One print or electronic copy may be made for personal use only. Systematic reproduction and distribution, duplication of any material in the paper for a fee or for commercial purposes, or modification of the content of the paper are prohibited.

With the wide variety of different material chemistries in use, it is important that the selection and optimization of filter and membrane types are reasonably simple to implement. Selection involves not only matching the type of membrane to the chemistry, but also correlating the proper pore size and the differential pressures associated with each.

Unfortunately, filter priming requires track downtime and a considerable amount of chemical waste. The chemical is used to displace air from the filter housing and membrane pore structure. By utilizing a two-stage technology dispense system, such as the Entegris IntelliGen® Mini system seen in Figure 1, the material can be either recycled back to the bottle after passing through the filter or sent directly to drain. Sending the material to drain is what significantly increases the cost of wasted material. By being able to recycle the material back to the bottle, the end user is able to save a significant amount of material and ensure its cleanliness.

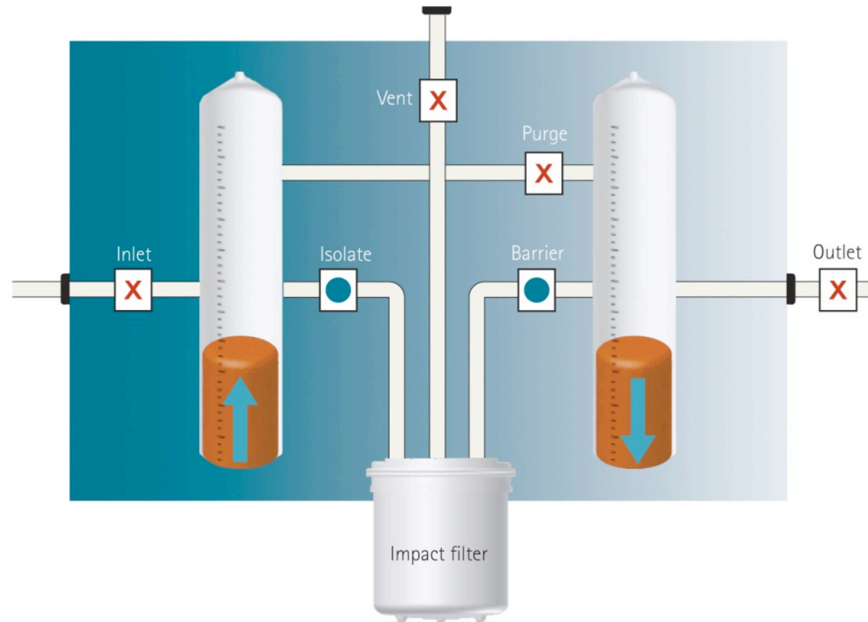

Figure 1. IntelliGen® Mini dispense system.

For material suppliers, the filter priming process is increasingly problematic. The rapid increase in lithography process techniques has increased the rate of chemical research and development. New materials are constantly being tested, which requires a chemical supplier to frequently change filters to accommodate new chemistries undergoing lithographic and defect performance studies. The frequency of filter changes at a material supplier is vastly increased over that of an end user. Therefore, it is important to provide time- and cost-saving measures to material suppliers in the research and development phase. Ideally these measures can be evaluated and passed along to the end user when the material is finally ready for manufacture and sale.

This paper will investigate the interaction between a single spin-on hardmask and various membrane materials, examining effects on defect type and density. By using an Entegris Intelligen® Mini dispense pump, various filtration settings will be used to determine the optimum conditions for each membrane, filter, and chemistry combination.

2. EXPERIMENTAL

As lithographic processes become more challenging, equipment and materials become increasingly expensive. It is important for chemical manufacturers to ensure that the materials produced for lithographic processes are clean and will perform immediately with minimal end user effort. A study was conducted to determine the optimum filter priming sequence for each filter, reducing track downtime and reaching baseline defectivity while using the minimum amount of

spin-on silicon-containing hardmask, or Si-HM. Each filter was installed using a recommended priming sequence.[1,2,3] Following the priming sequence, up to 3 liters of the Si-HM material was purged through the system, which included the pump, dispense lines, and dispense tip. After various volumes of material were purged, wafers were coated for on-wafer defect analysis. This analysis measured the effectiveness of the filter priming process with the Si-HM as well as the compatibility of the Si-HM and filter media.

The filter priming method utilized in this study is based on a recirculation methodology whereby the material is circulated through the filter and the feed and dispense chambers. While the Intelligen® Mini has a filter priming sequence function that can be manually loaded into its operating software, the method used in this study was a file upload option that allowed a previously programmed sequence saved in a file to be downloaded into the pump and be automatically run by the dispense system. Initial laboratory results showed that this method reduced the time to prime the filter by 60% when compared to the standard method.

Utilizing these priming sequences, OptiStack® HM825-302.6 hardmask material (Brewer Science) was installed on the IntelliGen® Mini system. During the purging testing, five consecutive wafers were coated on a TEL® Mark 8 coater to a final nominal thickness of 26 nm at a casting speed of 1500 rpm. The wafers were inspected using a dark-field inspection system with a 46-nm defect detection capability for the hardmask material. The Impact® 2 filters studied in this experiment included 10-, 5-, and 3-nm asymmetric and 10-nm symmetric UPE filters.

Once baseline defectivity levels were reached for each filter, a designed experiment (DOE) was conducted which examined the filtration pressure and filtration rate as factors. Each factor was tested at four levels that spanned the range of the acceptable settings for each filter type. Filtration pressure was varied from 2 to 8 psi, while the filtration rate was varied from 0.1 to 3 ml/s. The 3-nm filter was limited to a maximum of 2 ml/s due to the smaller pore size of the membrane. For each condition, five wafers were consecutively coated on a TEL® Mark 8 as described above and were inspected by the same dark-field inspection system.

3. RESULTS AND DISCUSSION

3.1 Baseline defectivity

In measuring a filter's effectiveness, fully wetting or passivating the filter is important. In this state, the filter should not pass defects or microbubbles through the membrane and will reach a baseline defect level upon the purging of a volume of the material through the membrane. The hold-up volume in the test setup from source bottle to dispense nozzle is approximately 250 mL. In this study it was assumed that the baseline defect level was reached when at least 10 times the hold-up volume, 2.5 L, had been purged through the system, thus creating a metric for comparison.

Figure 2 displays the defect count results of the priming and purging test. Results showed that a reduction in pore size of the filter directly correlated to lower defect counts on a wafer, especially for defects smaller than 80 nm. Each of the asymmetric filter types achieved a baseline that was proportional to its pore size, that is, the 3-nm filter yielded the lowest defect count, followed by the 5-nm filter count and then the 10-nm filter count. Testing with the 10-nm symmetric filter was stopped because of the higher defect counts. Also, the volume of material needed to reach the respective defect baselines is shown in Figure 2. Use of the smaller pore size allowed faster start-up due to overall lower baseline defect results. The 3-nm filter was ready for production almost immediately after priming, while the filters with larger pores required at least 2 liters of material to achieve an acceptable baseline. While there were subtle differences in the priming recipes, specifically the lower maximum filtration rate necessitated by the smaller 3-nm pore size, the Si-HM material not only appeared to wet the 3-nm membrane fully, but the 3-nm pore size was more effective at removing defects than the larger 5-nm and 10-nm pore sizes. Repeating the 3-nm priming process on the larger pore sizes would determine whether the filter priming sequence is the controlling factor for passivating and wetting the filter, or whether the filter pore size has the greater effect on defect reduction. These results also show that the use of filters with a smaller pore size during Si-HM manufacturing could allow better defect control and further reduction of coat defects at the end user site.

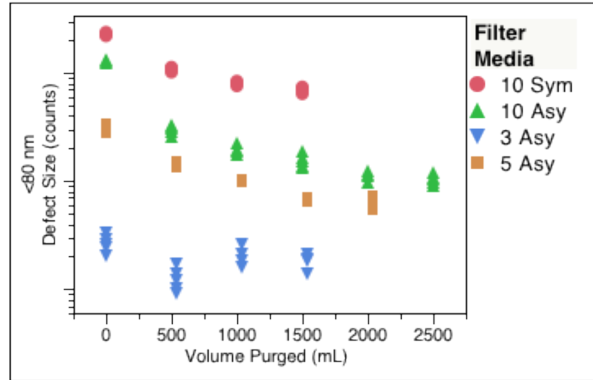

Figure 2. Coat defects smaller than 80 nm through purge volume.

Interestingly, when analysis of the purging trends through defect size was completed, a change in defect behavior was seen for defects smaller than 80 nm compared to defects greater than 80 nm for the asymmetric filters. Detected defects smaller than 80 nm showed a decrease with purge volume. Detected defects larger than 80 nm did not show the same trend. Figure 3 displays these results. The 10-nm symmetric filter does not exhibit this same behavior, again proving the effectiveness of the priming and wetting of the asymmetric filters, and confirming that non-ideal priming sequences will require much greater amounts of material to be purged than what is really necessary. Because all three asymmetric filters show the same behavior for defects larger than 80 nm, it is implied that the toolsets used to coat these materials are responsible for the remainder of the defects that are 80 nm and larger. Likewise, the filter is removing defects from the Si-HM at or below this 80-nm size break. These results imply the same arguments as stated earlier, that the Si-HM may have small defects inherent in the chemistry. Because chemical formulation changes usually require significant investments in time and testing to ensure that all product requirements (such as thickness, optical properties, etch rate, etc.) are still met, improved filtration during manufacture and end-use can be accomplished with no impact on other important product parameters.

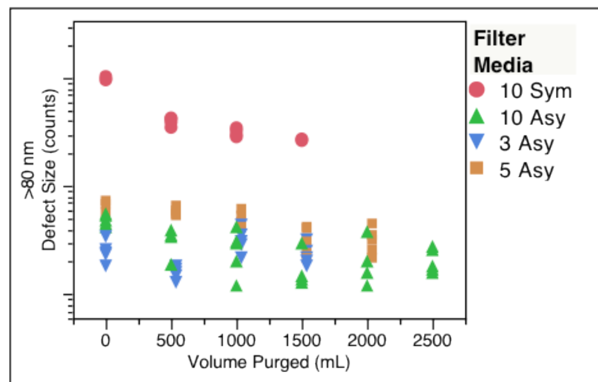

(a)

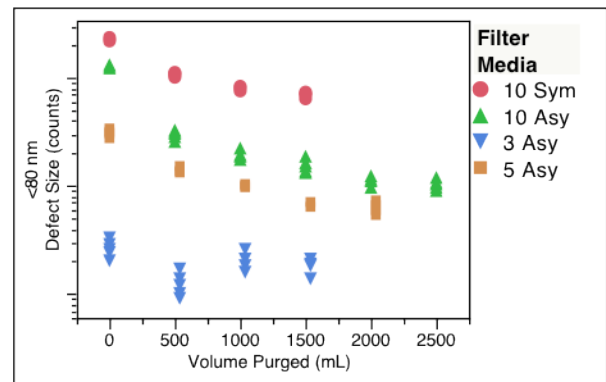

(b)

Figure 3. Defect counts through purge volume for (a) >80 nm defect size and (b) <80 nm defect size.

Filter media morphology is important as well. Recognizing the differences between the asymmetric and symmetric design is crucial to effectively filter the Si-HM material. By comparing the defect count differences between the 10-nm symmetric UPE and 10-nm asymmetric UPE in Figure 3, it was shown that the asymmetric morphology showed significantly lower defect counts compared to the symmetric design. Due to the vast difference in defect reduction, testing of the 10-nm symmetric filter was terminated after the results of this purging test were examined. A possible reason for the performance of the 10-nm symmetric is that the priming sequence is not optimized sufficiently yet for Si-HM materials, and the filter may not be completely wetted and passivated. Historical data have shown that when defects larger than 80 nm are not reduced after filter priming, the filter is not completely wetted or passivated and further

purging is required. The data for the 10-nm symmetric UPE showed this behavior; therefore, testing with that filter type was not continued.

3.2 Filtration Process Experimentation

Once the filters were primed and reached their respective baseline defect levels, a designed experiment was run to determine the effects of filtration process parameters such as filtration rate and filtration pressure on the defect count. The designed experiment for these two factors at four separate levels was developed and tested on each filter. The DOE was designed such that up to a quadratic term could be modeled to the data, thereby allowing a process window to be determined for the pump, filter, and Si-HM combination. Besides modeling defects counts, the wafer haze was modeled as well.

3.2.1 Coat Defect

To determine the strongest model parameters for any given filter, a simple failure mode type risk analysis was performed. A Pareto chart was created for each of the model factors for a given filter, for a quadratic model with two variables that would yield five modeling parameters. Once the model was determined for a given filter, the strength of the modeling parameters were ranked where the strongest model parameter was given a value of 5, and the weakest was given a 1. This ranking of the model parameters was repeated for each filter. Once the model parameters were ranked for every filter, the ranks of each model parameter were multiplied together. This multiplication step scaled the modeling terms that were significant to the defect count. The resultant Pareto chart for the risk analysis is shown in Figure 4. The two largest model terms accounted for 85% of the Pareto.

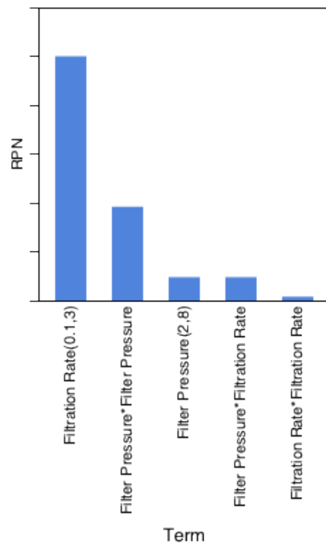

Figure 4. Risk Pareto chart of modeling terms for coat defects.

The strongest modeling term was the filtration rate. Using the IntelliGen® Mini system, it was easy to change the filtration rate because filtration and dispense operations are separate. Because this term is a single linear parameter that can be directly manipulated using the pump software, it was easy to adjust the filtration rate to the high and low extremes. Based on the model, it is assumed that this will yield lower defect results. In this way, the mini pump has an advantage over single-stage dispense pumps in that it may not be possible to vary the filtration rate without affecting the dispense rate of the fluid. Also, on some newer pump setups the pump draws the material through the filter at slow filtration rates. Therefore, the best filtration rate may be beyond the maximum filtration rate attainable with single stage pumps.

The next strongest modeling term was "Filter Pressure*Filter Pressure." This is a quadratic, higher-order term that will cause a parabolic curvature in the defect modeling. The filtration pressure can be changed easily on the IntelliGen® Mini system, but because of the curvature in the defect model due to this term, the pressure must be carefully set. Small deviations in the ideal pressure settings could yield significant changes in the defect response. Again, the IntelliGen® Mini system has an advantage in this area over other pump setups. On single-stage pumps where the filter is downstream from the pump, the dispense and/or stop-suckback valve will have to be adjusted to maintain filtration pressure at the desired dispense rate and volume. On other pumps where the filter is upstream from the dispense pump, another system may have to be installed to maintain the proper pressure across the filter. Whether that secondary system is direct air pressure on the fluid or some sort of diaphragm pump, under certain conditions these pumps could increase the chance of microbubbles or other type of defects.

Because the main model terms that affect defect counts have been determined, a more detailed analysis can be completed for each filter. Filtration rate, as stated previously, follows a linear trend line with the best factor setting either low or high. Other weaker model terms impart slight curvature to the filtration rate term; however, the overall linear trend is dominant. The results of that analysis are shown in Figure 5. For the 10-nm and 5-nm asymmetric filter design, higher filtration rates of up to 3 mL/s yielded a lower wafer defect count. For the 3-nm filter, there was no statistically significant (at 95% confidence) model term found during the analysis, hence the large blue error bars associated with the modeling of filtration rate. For the 3-nm filter, that finding implies that the background defect level of the coater is too high to see the changes during the experiment, or the filter has a very wide operating window and will work effectively on the IntelliGen® Mini across the range of settings examined in this experiment. However, if the trend line is to be believed, then a low filtration rate would be preferred. Physically, this would be correct as the small pore size would in general make it more difficult to push material through the membrane, and higher filtration rates would create a situation where the differential pressure across the membrane would increase. This pressure increase not only could possibly cause pump or filter problems, but would likely cause higher defect counts.

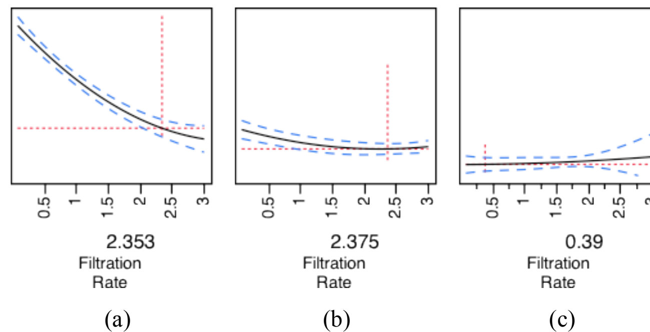

Figure 5. Detailed results of coat defects with filtration rate for the (a) 10-nm, (b) 5-nm, (c) 3-nm asymmetric filters. Settings shown are at or near best case for lowest defects.

When the weaker effect of filtration pressure was examined, the 3-nm filter again did not have a statistically significant model term (at 95% confidence), yielding error bars which were quite large, indicating a large processing window for the 3-nm filter based on the results of this experiment. Again, if the trendline is followed for the 3-nm filter, then keeping the filtration pressure low is preferred. The filtration pressure terms have a large curvature in the results, which can be seen in Figure 6. For the 10-nm filter, a low filter pressure is ideal, while for the 5-nm filter a setting of moderate filtration pressure is optimum. These pressure settings help bolster the hypothesis that the Si-HM has a high amount of extremely small defects that are only removed using filters with the smallest pore size. If larger pore sizes are used at the wrong settings, these defects could be pushed through the filter and onto the wafer, thus creating defects. At the optimum settings, some of these extremely small material defects could be caught by the filter.

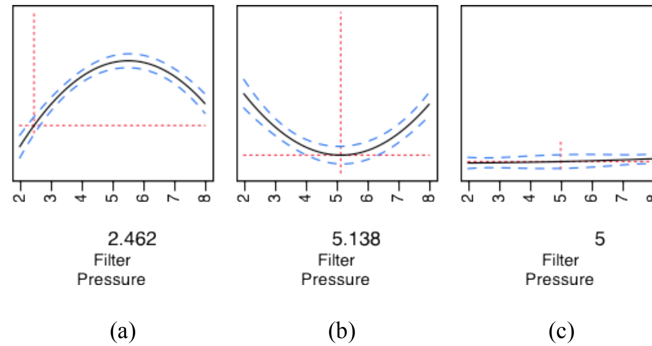

Figure 6. Detailed results of coat defects with filtration pressure for the (a) 10-nm, (b) 5-nm, (c) 3-nm asymmetric filters. Settings shown are at or near best case for lowest defects.

3.2.2 Haze Analysis

Haze is the measurement of the background noise light scattering from the wafer as detected by the defect inspection system. This background noise will affect the signal-to-noise ratio of the defect and therefore the minimum defect size detected by the tool. For the defect tool used in this study, a minimum signal-to-noise ratio of 2.0 was used to determine the minimum defect size possible for the Si-HM, which was 46 nm. Analysis of the haze was completed along with the defect analysis to determine if the haze changed during the purging test or the filtration DOE. If the haze does change with filter type or filtration process, that correlation may have an effect on the minimum defect size through a change in the signal-to-noise ratio. Such a finding would allow the defect tool to have the greatest sensitivity and be able to detect the smallest defects at the minimum signal-to-noise ratio acceptable for the defect tool. The analysis followed the same procedure as the coat defects. A Pareto chart was used to determine the strongest modeling terms, followed by a detailed analysis for those modeling terms for each filter.

The “Wide” and “Narrow” channels of the defect tool were analyzed separately, and the results are shown below in Figure 7. One impact of reducing the pore size of the filter is that the overall haze was reduced, making it possible to reduce the haze in general and increase the sensitivity of the tool. In both channels, the modeling term “Filter Pressure*Filtration Rate” is the most significant. Because this term is the most significant, it does not allow for simultaneous reduction of both haze and defect count, so a trade-off must be considered while optimizing for ultimate defect sensitivity or ultimate defect count. For example, if the end user optimized for ultimate defect sensitivity, or lowest haze, the baseline defect count may be 20-30% higher, assuming the minimum defect size did not change. Therefore careful consideration must be made as to which mode should be used to optimize defectivity. Usually the Wide channel of the defect tool is used to determine ultimate defect size resolution. Therefore, the Wide channel Pareto chart was used for detailed analysis, where the next important modeling term is filter pressure.

Assuming that optimizing haze is the goal, the detailed analysis by filter size shows a solution for each filter. The Wide channel results are shown in Figure 8. The 10-nm filter haze results were exactly the opposite of the defect results. Previously, the defect results indicated low filter pressure and high filtration rate would yield the lowest defect results.

For the 10-nm filter, the trade-off between ultimate resolution and lowest coat defects must be weighted and considered. The 5-nm filter results showed no significant modeling terms for haze. Therefore the 5-nm filter can be optimized for both ultimate resolution and the ultimate low-defect coating. The same results summary can be said for the 3-nm filter. For the 3-nm filter, the haze can be optimized for high filtration rate and high filtration pressure, but if the trend lines in the defect data are to be believed, then these settings for best haze would be opposite those needed for low defects.

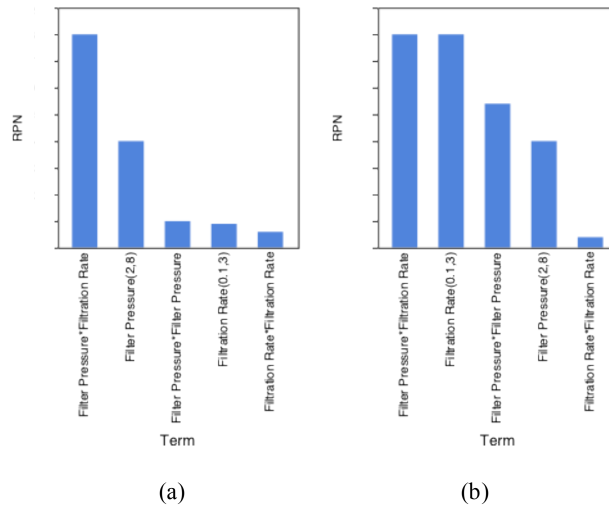

Figure 7. (a) Wide and (b) Narrow channel haze risk Pareto chart.

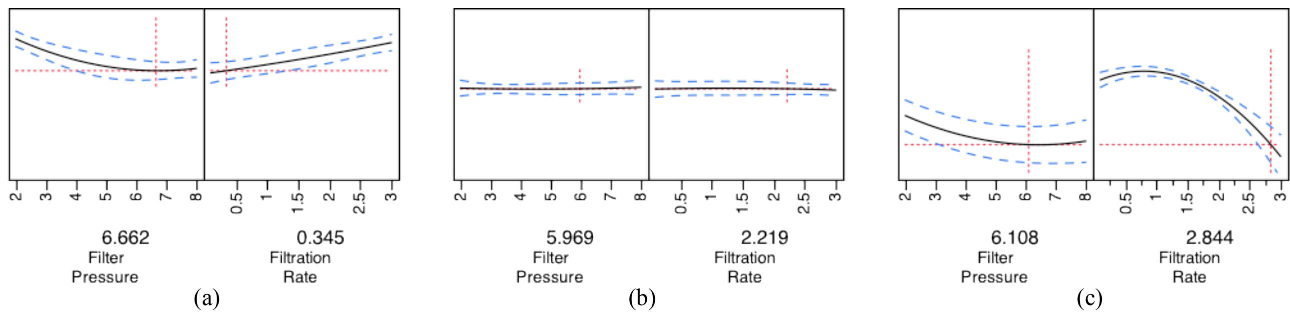

Figure 8. Detailed results of Wide haze with filtration pressure and rate for the (a) 10-nm, (b) 5-nm, (c) 3-nm asymmetric filters. Settings shown are at or near best case for lowest haze.

4. CONCLUSION

As device manufacturers continue to strive for higher-yielding wafers and increased productivity, it becomes clear that defects during wafer coating pose a significant challenge. During product development in chemical manufacturing, a clear understanding of filter interactions that can occur will enhance future product evaluations. As shown in this paper, proper filter priming with the proper purging process will yield quicker startup. Results showed that a reduction in pore size of the filter directly correlated to lower defect counts on a wafer, especially for defects smaller than 80 nm. Each of the asymmetric filter types achieved a baseline that was proportional to its pore size, that is, the 3-nm filter yielded the lowest defect count, followed by the 5-nm and then the 10-nm filters.

In addition, end users can improve their processes by understanding the differences between filter membranes and their interactions with specific chemicals. As filter pore sizes decrease, proper filtration settings must be used to ensure low-defect coatings. A second order polynomial fit of defect data for the factors of filtration rate and filtration pressure was completed. The strongest modeling parameter was the filtration rate followed by "Filter Pressure*Filter Pressure" for the asymmetric filters having the larger pore sizes; the 3-nm filter showed no dependence on any modeling parameter within 95% confidence limits of the test.

These filtration settings also have an effect on the background noise or haze of the defect measuring tool. As with defects, the haze was lowered with smaller-pore-size filters, allowing for a possible increase in defect sensitivity. Utilizing the same polynomial fit for haze as for defects, in both the Wide and Narrow channels the modeling term "Filter Pressure*Filtration Rate" was the most significant. Because this modeling term is not the same as it was in reducing defects, a trade-off may be made between ultimate defect count and lowest haze values in order to increase sensitivity of the defect tool. Careful consideration of the defect detection recipe should be considered as filtration changes are made to pump and coating processes.

ACKNOWLEDGEMENTS

The authors would like to thank Michael Weigand and Brian Smith of Brewer Science, Inc., for management support of this study, and Jennifer Braggin and Brent Bjorneberg of Entegris for helpful technical discussions.

REFERENCES

[1] Batchelder, T., "Optimized filter priming method to minimize maintenance downtime," Entegris, Inc., Applications Note 3811-2706 (2006).
[2] Wu, A., and Chow, W., "A technique for rapid elimination of microbubbles for photochemical filter startup," *Proc. SPIE*, 7140, 71402Y (2008).
[3] Batchelder, T., and Braggin, J., "Priming method for IntelliGen Mini," Entegris, Inc., Applications Note 3811-5352 (2007).